Structural Studies of Nanophase-Separated Poly(2-hydroxyethyl methacrylate)-*l*-polyisobutylene Amphiphilic Conetworks by Solid-State NMR and Small-Angle X-ray Scattering

Attila Domján,[†,‡] Gábor Erdödi,[†] Manfred Wilhelm,[‡] Michael Neidhöfer,[‡] Katharina Landfester,[‡] Béla Iván,*[,†] and Hans Wolfgang Spiess*[,‡]

Department of Polymer Chemistry and Material Science, Institute of Chemistry, Chemical Research Center, Hungarian Academy of Sciences, H-1525 Budapest, Pusztaszeri u. 59-67, P.O. Box 17, Hungary, and Max Planck Institute for Polymer Research, P.O. Box 3148, D-55021 Mainz, Germany

Received June 28, 2003; Revised Manuscript Received September 19, 2003

ABSTRACT: Bicomponent nanophase-separated poly(2-hydroxyethyl methacrylate)-*linked*-polyisobutylene (PHEMA-*l*-PIB) amphiphilic conetworks were synthesized by radical copolymerization of methacrylate−telechelic polyisobutylene (MA−PIB−MA) and different amounts of 2-(trimethylsilyloxy)ethyl methacrylate (SEMA) followed by quantitative hydrolysis of the trimethylsilyl protecting groups. The PIB content of the resulting conetworks, determined by elemental analysis and solid-state ^{1}H NMR under fast magic-angle spinning (MAS), varied between 17 and 63% w/w. Phase separation and morphology of these conetworks were investigated by DSC, small-angle X-ray scattering (SAXS), and for the first time by ^{1}H spin diffusion solid-state NMR. Two T_g values were observed by DSC in all samples. The observed T_g values were close to the literature values of both homopolymers (110 °C for PHEMA and −67 °C for PIB), indicating a strong phase-separated morphology in these conetworks. Parameters were optimized for the ^{1}H spin diffusion NMR experiments, and the measurements were carried out with six filtering cycles and a 10 μs delay between pulses at 90 °C. The NMR and SAXS measurements prove strong phase-separated morphology. The sizes of the hydrophilic (PHEMA) and hydrophobic (PIB) nanodomains were determined to be in the 5−15 nm range. The spin diffusion experiments also indicate strongly separated phases without a detectable interface with mixed components. The long period of our system seems to depend weakly on the volume fraction whereas the morphology of the nanophases depends on the volume fraction.

Introduction

Well-defined heterogeneous polymeric architectures have played an important role in polymer chemistry and technology in recent years (see e.g. refs 1−5 and references therein). One type of these promising materials belongs to amphiphilic conetworks (see Scheme 1) which exhibit several unique advantageous properties. The synthesis of these new bicomponent polymeric architectures relies on the availability of well-defined telechelic polymers, such as polyisobutylene with predetermined molecular weight (MW) and a narrow molecular weight distribution (MWD) obtained by quasi-living carbocationic polymerization.[6−10] The synthetic difficulties originate mainly from macroscopic phase separation during the preparation of the conetwork that occurs due to the incompatibility of the polymers. Systematic research in this field has only started in recent years.[7,11−29]

The amphiphilic conetworks are bi- or multicomponent polymeric materials which contain covalently bonded immiscible hydrophilic and hydrophobic polymer chain segments. This yields unique nanostructured composites with cross-linked but nanoseparated morphology.[21,31] The solubility parameters of the two polymers are usually very different in amphiphilic conetworks so that the components do not mix, but macroscopic phase separation is hindered by the covalent bonds between them. As a consequence of the network structure, the phase separation is only possible in the microscopic range, and therefore, the conetworks are macroscopically homogeneous. This results in a special bulk and surface structure which was confirmed for few cases by transmission electron microscopy (TEM),[21,30] atomic force microscopy,[14,21] X-ray photoelectron spectroscopy,[14] small-angle X-ray scattering,[13,21] small-angle neutron scattering,[31] and solid-state NMR experiments[32] for certain conetworks. The amphiphilic conetworks swell in both hydrophilic and hydrophobic solvents[11,17,18,27,28] due to their amphiphilic character. Earlier investigations of certain amphiphilic conetworks, such as poly(2-hydroxyethyl methacrylate)-*l*-polyisobutylene, poly(*N*,*N*-dimethylacrylamide)-*l*-polyisobutylene, and poly(*N*,*N*-dimethylaminoethyl methacrylate)-*l*-polyisobutylene (*l* stands for covalently linked),

Scheme 1. Structure of Monomers (IB = Isobutylene, HEMA = 2-Hydroxyethyl Methacrylate, SEMA = 2-(Trimethylsilyloxy)ethyl Methacrylate) and Methacrylate−Telechelic Polyisobutylene MA−PIB−MA Macromonomer

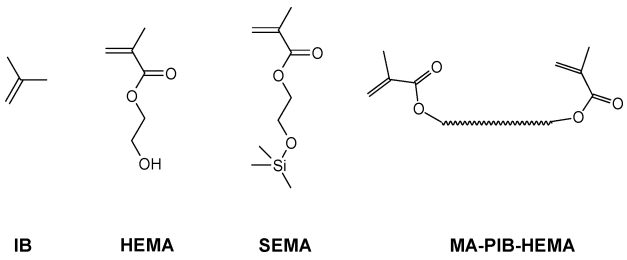

* Corresponding Authors. B.I. E-mail: bi@chemres.hu. Telephone: +36-1-325-9033. Fax: +36-1-325-7898. H.W.S.: E-mail: spiess@mpip-mainz.mpg.de. Telephone: +49-6131-379120. Fax: +49-6131-379320.

† Hungarian Academy of Sciences.

‡ Max Planck Institute for Polymer Research.

10.1021/ma034891h CCC: $25.00
Published on Web 11/07/2003

Table 1. Synthesis Parameters of the Preparation of PHEMA-*l*-PIB Amphiphilic Conetworks[a]

sample	W_{PIB}[b] [% w/w]	m_{PIB} [g]	V_{SEMA} [cm^3]	m_{SEMA} [g]	n_{SEMA} [mmol]	$V_{AIBN\ stock}$ [cm^3]	n_{AIBN} [μmol]	V_{THF} [cm^3]
1	35	0.70	2.18	2.02	9.99	2.00	20.0	3.05
2	40	0.80	2.01	1.87	9.22	1.84	18.4	3.26
3	45	0.90	1.84	1.71	8.45	1.69	16.9	3.47
4	50	1.00	1.68	1.55	7.68	1.54	15.4	3.68
5	70	1.40	1.01	0.93	4.61	0.92	9.2	4.52
6	75	1.50	0.84	0.78	3.84	0.77	7.7	4.73
7	80	1.60	0.67	0.62	3.07	0.61	6.1	4.94
8	85	1.70	0.50	0.47	2.31	0.46	4.6	5.15

[a] The following values are constant for all samples: $(m_{PIB} + m_{SEMA})/V_{all\ component} = 0.25$ g/cm^3; $m_{PIB} + m_{HEMA} = 2.0$ g; $n_{SEMA}/n_{AIBN} = 500$ (W = weight %, m = mass, V = volume, n = mole). [b] The values were calculated from the data used for preparation.

with around 50/50 w/w % hydrophilic/hydrophobic composition have shown that they are biocompatible[33] and blood compatible[34] materials. The very mobile PIB chains give flexibility to the amphiphilic conetworks, and they are generally rubbery materials depending on the PIB content.[13] In the swollen state, conventional hydrogels of cross-linked homopolymers lose mostly their mechanical stability, and in the highly swollen state, their structure can disintegrate. In the amphiphilic conetworks, the hydrophilic phases are covalently bonded in the network structure with double covalent linked PIB chains, which prevent the disintegration. The PIB chains provide the conetworks toughness and additionally an upper limit of the swelling ratio, which decreases the possibility of disintegrating the structure. These favorable properties and the nanoseparated morphology make the PIB-based amphiphilic conetworks promising candidates in nanoscience as matrix materials for building separated inorganic nanoparticles[21] and in medical applications as implants and controlled drug release matrices.[7,11,12,28,35,36]

In this work we have systematically investigated the structure of a poly(2-hydroxyethyl methacrylate)-*l*-polyisobutylene (PHEMA-*l*-PIB) amphiphilic conetwork series with different hydrophilic−hydrophobic polymer content. The conetworks were synthesized by free radical copolymerization of methacrylate−telechelic polyisobutylene (MA−PIB−MA) and SEMA followed by quantitative deprotection as described earlier.[7,28,36] The chemical composition of the conetworks was determined by elemental analysis and solid-state ^{1}H NMR under fast MAS. According to previous work,[13,21] the PHEMA-*l*-PIB amphiphilic conetwork contains domains with an average size of several nanometer, but further systematic morphological studies are not yet available.

For medical and nanotechnological applications it is very important to characterize and understand the underlying morphology and determine the size of the nanodomains within the amphiphilic conetworks. These structural properties should highly influence the swelling properties of the conetworks in different solvents and other physical and chemical properties. The existence of a strong phase separation was indicated by differential scanning calorimetry (DSC).[7,28] Various solid-state NMR techniques can be used for the characterization of complex polymeric structures (see e.g. refs 37−46). Because of the strong phase separation and well-defined structure of the investigated amphiphilic conetworks, the ^{1}H spin diffusion solid-state NMR technique is one of the most powerful methods to determine phase separation in the nanometer range, specifically for ill-defined structures.[37−42,44−49] The structure of amphiphilic conetworks is macroscopically homogeneous, but short-range order was found by small-angle neutron scattering (SANS) measurement.[31] In this study the size of the nanophases and the underlying morphology of the chemically generated nanostructure of these bicomponent covalent conetworks are characterized by ^{1}H spin diffusion solid-state NMR and small-angle X-ray scattering (SAXS).

Experimental Section

Materials. 2-(Trimethylsilyloxy)ethyl methacrylate (SEMA) (Aldrich) was freshly distilled, and AIBN (Aldrich) was recrystallized twice from methanol before use. Solvents were used as received, except THF which was freshly distilled from $LiAlH_4$. The synthesis of the methacrylate−telechelic PIB (M_n = 5000 g/mol, M_w/M_n = 1.01, functionality = 2.0) has already been described elsewhere.[7,28,36]

Synthesis of Poly(2-hydroxyethyl methacrylate)-*l*-polyisobutylene (PHEMA-*l*-PIB) Amphiphilic Conetworks. The preparation of PHEMA-*l*-PIB amphiphilic conetworks using protected hydrophilic monomer and polymeric PIB cross-linker has already been described in a previous work,[7] and the synthetic procedure given here is the same with only minor differences (see below). The two different monomers and the macromonomer used for this study are shown in Scheme 1. One of the changes in the synthetic procedure is the variation of the initiator concentration ([I]) relative to the monomer concentration ([M]). Previously [I] was always chosen to be proportional to [M]^2 in order to attempt to polymerize the hydrophilic monomer (in particular the SEMA) with a constant chain length in the whole series of the conetworks with different compositions. In our study, [I] was changed linearly with [M] because the kinetics of the free radical polymerization in a network formation reaction after the gel point usually cannot be described by the equation based on the above-mentioned relation:[28] $1/DP_n = \text{const}\cdot[M]/([I])^{1/2}$. Therefore, [I] was chosen such that the synthesis resulted in the longest possible hydrophilic chains. Practical aspects of the synthesis might also be important: e.g., to avoid low monomer conversion (at low [I]), formation of bubbles (too high [I]), etc.

The amphiphilic conetwork samples were prepared using a linear variation of [I] with respect to [M]. The parameters of the synthesis (the specific amounts of the reactants and solvents) are listed in Table 1.

The desired amounts of methacrylate−telechelic PIB (MA−PIB−MA) were measured into a 50 cm^3 reaction flasks. The flasks with MA−PIB−MA, trimethylsilyloxyethyl methacrylate (SEMA), AIBN stock solution in THF (c = 0.01 M), and THF was placed into a glovebox filled with N_2. The appropriate amounts of SEMA, AIBN stock solution, and THF were weighed into glass vessels. The mixtures were homogenized with magnetic stirring bars and transferred into hollows of a Teflon mold. Then the mold was hermetically sealed. Afterward, it was removed from the glovebox and placed into an oven and kept there at 60 °C for 3 days. Then, the mold was allowed to cool before opening. The networks were allowed to dry in air for 2 days, and then the cross-linked samples were placed into HCl solutions (c = 0.01 M) of ethylene glycol methyl ether/methanol (50:50) mixture, followed by methanol and methanol/water mixture (50:50) to eliminate the protecting groups. The networks were immersed into these solutions

Table 2. Results of Elemental Analyses, ^{1}H MAS NMR, and DSC Measurements of PHEMA-*l*-PIB Amphiphilic Conetworks

sample no.	PIB [% w/w] (elemental analysis)	PIB [% w/w] (^{1}H MAS NMR)	PHEMA [% w/w] (elemental analysis)	PHEMA [% w/w] (^{1}H MAS NMR)	T_g of PIB [°C]	T_g of PHEMA [°C]
1	17	10	83	90	-63	111
2	24	15	76	85	-61	109
3	26	18	74	82	-60	108
4	28	26	72	74	-60	107
5	50	34	50	66	-59	102
6	57	52	43	48	-56	102
7	57	54	43	46	-57	100
8	63	62	37	38	-55	96

Scheme 2. Proposed Structure of PHEMA-*l*-PIB Amphiphilic Conetworks, Specifically for Low PIB Content Where Spherical PIB Structures of Roughly 15 nm Diameter Dominate the Morphology

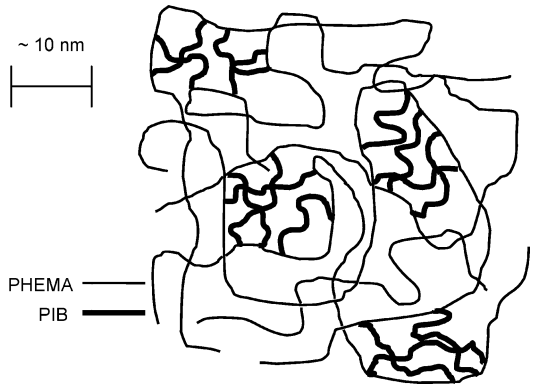

sequentially for 5 days. The HCl solutions (150 cm^3) were exchanged with fresh solutions daily. Then the samples were immersed into methanol for 3 days and subsequently into hexane for 3 days. The resulting materials were allowed to dry in air for 3 days, and further drying was made in a vacuum until constant weight (1 day at room temperature and 5 days at 130 °C) was reached.

The architecture of the prepared amphiphilic conetworks is determined by the starting materials of the conetwork formation. Scheme 2 shows the designed materials containing chains with opposite miscibility connected covalently to each other. The PIB chains are bridging between the PHEMA chains and have narrow MWD; i.e., $M_{c,PIB}$ can be regarded as constant ($M_{c,PIB}$ = 5000 g/mol) throughout the conetwork structure of any sample in the whole series of the conetworks. On the other hand, $M_{c,PHEMA}$ has a broader distribution than $M_{c,PIB}$, and it changes with composition. Since the overall crosslink density (D_{cr}) originates from these particular quantities, each member of the series of conetworks will possess a different D_{cr}, which increases with the PIB content of the amphiphilic conetworks.

Elemental Composition. The compositions of amphiphilic conetworks were determined by elemental analysis and checked by single-pulse ^{1}H fast MAS solid-state NMR spectra ($\omega_R/2\pi$ = 25 kHz, 700 MHz spectrometer). The peak in the ^{1}H spectrum at 3.9 ppm is related to the two O−CH_2 segments of PHEMA, and the peak at 1.1 ppm is related to protons originating from both PIB and PHEMA (spectra not shown). Peak integration yielded the relative content. The results are listed in Table 2.

The PIB content of the samples determined by NMR is generally 5−10% w/w smaller than the results of the elemental analysis, and the difference is independent of the PIB content. Because of the complexity of the investigated system, the reason for these slight differences is not obvious, and further investigations are needed along this line.

^{1}H Spin Diffusion Solid-State NMR. All NMR experiments were performed on a Bruker DSX spectrometer, operating at ^{1}H frequency of 300.22 MHz (7.05 T) with a commercial 7 mm static double-resonance probe. To select the magnetization of the mobile components and to selectively destroy the magnetization in the rigid phase, a dipolar filter[37−39,41,47,48] was used similar to a classical Goldman−Shen experiment.[49] The dipolar filter destroys the magnetization of the rigid phase with high T_g, but the magnetization is retained in the mobile phase. The 90° pulse length was 3 μs, and the spacing between the 90° pulses during the dipolar filter was set to 10 μs. After application of a dipolar filter, the magnetization was stored on the $\pm Z$ axis (parallel to the magnetic field B_0) for a mixing time t_m, during which ^{1}H spin diffusion occurs. Thereby, magnetization of the mobile PIB phase migrates to the rigid PHEMA phase until an equilibrium of magnetization is reached, i.e., for sufficiently long mixing times t_m. A read-out pulse returns the magnetization to the transverse plane where the signal of the magnetization is detected. The intensity of the highest peak in the ^{1}H spectra was taken for every mixing time. Afterward, the experimental data must be corrected for the T_1 relaxation which also reduces the intensity of the PIB signal in addition to ^{1}H spin diffusion. The T_1 relaxation decay was first separately measured for similar mixing times, t_m, without application of the dipolar filter, such that the magnetization decay is mostly caused by T_1 relaxation. The decay curves including dipolar filter and the various mixing times are influenced by both ^{1}H spin diffusion and T_1 relaxation. Consequently, these decay curves were corrected for the prior determined T_1 relaxation at each mixing time t_m. This is described in detail in refs 39 and 41. To acquire the spectra, a dead time delay of 5 μs and a spectral width of 150 kHz with a 3.35 μs dwell time were used.

The measurement of the T_2 transverse relaxation time is needed to estimate the spin diffusion coefficient[38,39] of the mobile phase. The detection of the T_2 transverse relaxation was obtained using a Carr−Purcell−Meiboom−Gill (CPMG)[52,53] sequence. All NMR experiments were carried out at 90 °C, that is, about 150 °C above the T_g of PIB and about 15 °C below the T_g of PHEMA to maximize the dynamical contrast between the two phases. Because of this high temperature, the option of using a solid echo for the determination of T_2 of PIB was discarded. Line width studies and T_2 measurements where within 10% deviations. Furthermore, it is important to mention that the size of the determined nanophase depends only on the root of the diffusion coefficient and hence is less sensitive to experimental errors of T_2. We consider the uncertainty of "ϵ" as the major source of inaccuracy.

Small-Angle X-ray Scattering (SAXS). The SAXS measurements were performed in an evacuated compact camera (Anton Paar KKK). As X-ray source, Cu Kα radiation with a wavelength of λ = 0.154 nm was used. The scattered intensity was recorded by a scintillation counter in a step-scanning mode. The samples were heated to 130 °C in a vacuum for one night to eliminate any water absorbed from the air before solid-state NMR and SAXS measurements were conducted.

Results and Discussion

DSC Investigations. The glass transition temperature T_g of bicomponent polymeric systems depends on the size of the heterogeneity, especially for small domains.[54,55] If the polymer components are immiscible, the sample exhibits two T_g's which can be associated with the different microphases. The difference in the T_g compared to the T_g of the pure material can be associated with the size and/or perfection of the phase

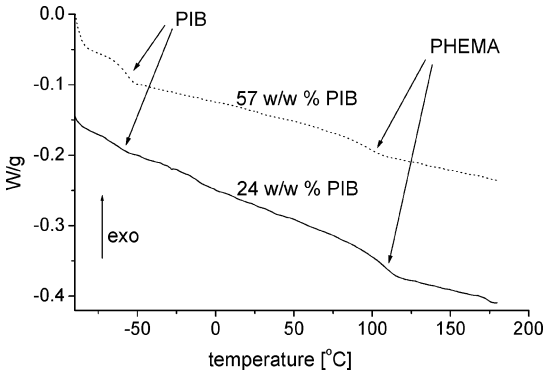

Figure 1. DSC curves of PHEMA-*l*-PIB amphiphilic conetworks containing 24% w/w (solid line) and 57% w/w polyisobutylene (dotted line).

separation. For our samples, two T_g's were observed (Figure 1), and the measured glass transition temperatures are very close to the literature values (Table 2) of the respective pure components in each case (−67 °C for PIB and 100−110 °C for PHEMA),[7,13,56] indicating strong phase separation of fairly pure PIB and PHEMA in PHEMA-*l*-PIB conetworks. The T_g of PHEMA decreases approximately linear while the T_g of PIB linearly increases with increasing PIB content in the conetworks. This phenomenon and the difference between the T_g's of the pure homopolymers and the components of conetworks will be discussed in detail elsewhere.[57]

^{1}H Spin Diffusion Investigations. Information on the domain sizes of the cross-linked polyisobutylene nanophases in amphiphilic conetworks was obtained by ^{1}H spin diffusion solid-state NMR experiments. The appropriate choice of temperature and strength of the dipolar filter as varied by the number of cycles and time separation between consecutive 90° pulses of the dipolar filter are crucial to the spin diffusion experiments. Because these amphiphilic conetworks are not only physical but also chemical networks, both PIB chains ends are covalently bonded to the high-T_g PHEMA, and the PIB chains should exhibit a mobility gradient similar to that of block copolymers.[58] As a consequence, the detected size of the very mobile PIB nanodomains, e.g., as seen by NMR, could be smaller than the size as found by scattering techniques (SAXS, SANS) or microscopy (AFM). If this effect exists, it will decrease with increasing temperature. To maximize the mobility contrast between the two polymeric phases and the underlying characteristic time (10−100 μs) of the segmental motion, 90 °C was chosen as measuring temperature in all cases. This temperature is just below the T_g of the rigid-state PHEMA (about 100−110 °C) and much higher than the T_g of the mobile-phase PIB (about −60 °C). The mobility difference between the mobile and the rigid-state components is clearly visible in the static single-pulse ^{1}H spectra of two amphiphilic conetworks with different PIB contents, as shown in Figure 2. The homogeneous ^{1}H line width can be correlated to the mobility of the PIB component. The rigid PHEMA has a broad peak (≈50 kHz fwhm), and the mobile PIB has a narrow peak (≈2 kHz fwhm).

The spin diffusion decay curves, as a function of the square root of mixing time, contain three important parameters:[39,41] the plateau value, the slope of the initial part, and the intercept of the extrapolated initial slope. The choice of the strength of the dipolar filter can be optimized via the plateau value. Furthermore, deviations from the stoichiometric ratio contain information about mobilization or immobilization of the two phases. The linearity of the decay of the first points vs $\sqrt{t_m}$ contains information about the interface or transitional region between different phases, and the slope reflects the average domain size of the mobile nanophase.[38,41,59]

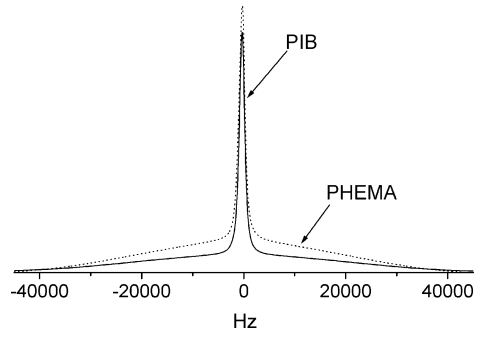

Figure 2. ^{1}H static NMR spectra of amphiphilic conetwork samples with different compositions. The solid line marks the spectra of the 63% w/w and the dotted line the 24% w/w PIB containing sample.

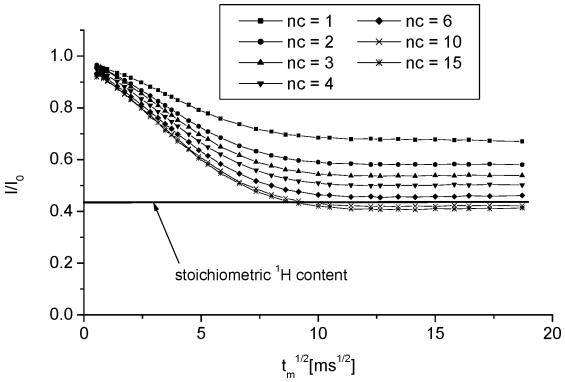

Figure 3. ^{1}H spin diffusion curves of PHEMA-*l*-PIB amphiphilic conetwork containing 28% w/w PIB, measured at 90 °C with different numbers of dipolar filter cycles (nc) with 10 μs spacing between the pulses. The plateau value is 0.43 (43% of protons are mobile), and it corresponds to the relative amount of PIB protons within the total amount of protons in the sample.

After a sufficiently long mixing time, t_m, the spin diffusion process is completed and the magnetization is equilibrated. The magnetization distribution between both phases finally becomes equal again. Consequently, beyond this point, the spin diffusion curve ideally reaches a horizontal plateau value representing the equilibrium magnetization of the system. The stoichiometric proton ratio of the "mobile" and "rigid" protons can be calculated from the number of the protons of the PIB and PHEMA phases and should, in a first approximation for a perfect phase separated system, be equal to the plateau value as detected by spin diffusion measurements.[41] The parameters that define the strength of the dipolar filter, such as the number of the filtering cycles and the delay between consecutive 90° pulses, have to be chosen carefully. If the dipolar filter is too weak, partial magnetization of the rigid phase remains, whereas if the filter is too strong, then some magnetization of the mobile phase will be destroyed. Hence, the obtained domain size will be either larger or smaller than the real one. Therefore, optimization of the dipolar filter strength is important.

Figure 3 shows the spin diffusion curves of the sample containing 28% w/w PIB at 90 °C with different num-

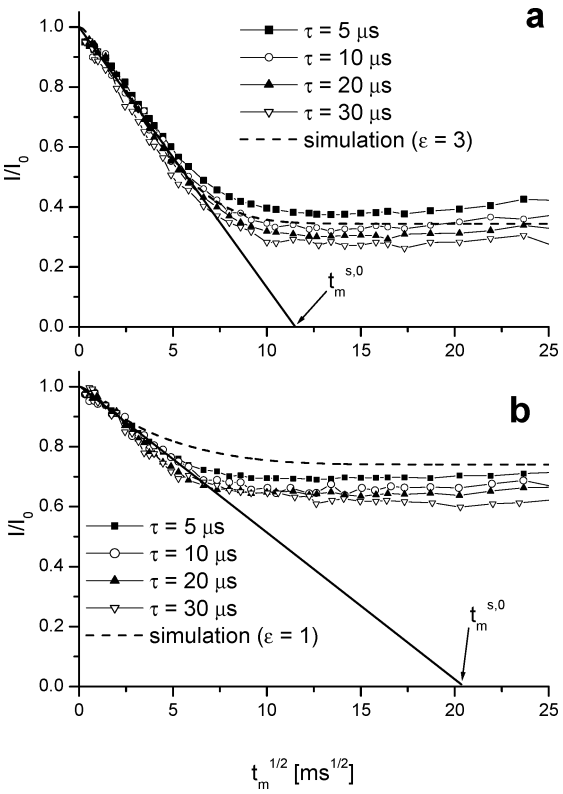

Figure 4. Spin diffusion curves of PHEMA-*l*-PIB amphiphilic conetworks at 90 °C with six cycles of dipolar filter and variation of the spacing between the pulses. A computer simulation of the decay of the magnetization is also included. For the simulation the following parameters were used: D_{mobile} = 0.07 nm²/ms, D_{rigid} = 0.8 nm²/ms, and d_{mobile} was calculated from the intercept of the extrapolated initial slope of the measured spin diffusion curve. The plateau value was calculated from results of the elemental analysis. The simulation agrees very well with the measured curve with 10 μs spacing for the 24% w/w PIB containing sample (a). For the 63% w/w PIB containing conetwork the measured plateau value is about 10% lower, but the initial slopes of the curves are the same (b).

bers of cycles of the dipolar filter with 10 μs spacing between the 90° pulses. This figure demonstrates the effect of the variation of the number of filtering cycles. In this sample, the mobile/total proton ratio is 0.43, which corresponds roughly to the plateau value of the spin diffusion curve obtained with six filter cycles. Note that the spin diffusion decay vs $\sqrt{t_m}$ is remarkably linear for the first points. Thus, the two phases of the conetworks are clearly separated; an interphase is not detected by NMR. The other parameter that regulates the strength of the dipolar filter is the spacing between the 90° pulses. Figure 4 shows the results of varying the spacing compared with simulations (six filtering cycles were used for the measurements). The parameters for the simulation were obtained from the solid-state NMR measurements (diffusion coefficient D_{mobile} and diameter of the mobile phase d_{mobile}), and the potential plateau value was calculated from the composition determined by elemental analysis.

For the conetwork containing 24% w/w PIB, the simulated and the measured spin diffusion curve with 10 μs spacing agree very well (Figure 4a). For the conetwork containing 63% w/w PIB, the plateau values of the simulation and the measurements differ by 15%, but the initial slopes of the curves, and thus their intercept, are similar (Figure 4b). The spacing between

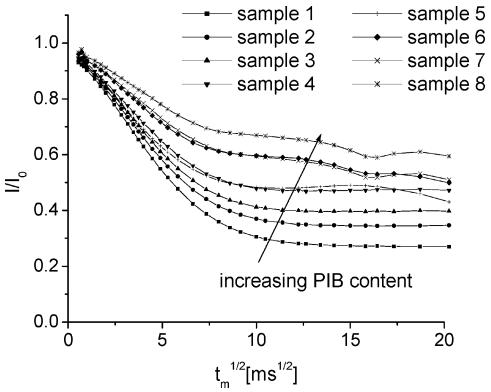

Figure 5. Spin diffusion curves of PHEMA-*l*-PIB amphiphilic conetworks at 90 °C with six cycles of the dipolar filter and 10 μs delay between the pulses. The initial slope of the curves and the plateau values change systematically for the PIB content of the samples. The arrow indicates the increase in PIB content.

pulses has a smaller effect on the intercept of the initial slope than the number of cycles in the investigated amphiphilic conetworks. To get comparable results, in all further ^{1}H spin diffusion experiments six filtering cycles and 10 μs delays between the pulses were used.

The spin diffusion curves of amphiphilic conetworks with different compositions are shown in Figure 5. The initial part of each curve is approximately linear, consistent with strong phase separation, which is in agreement with the results of the DSC measurements. The linearity of the initial region indicates that the opposing miscibility phases are separated from each other without any substantial interphase between them. The intercept of the initial slope of the first linear points of the curves ($\sqrt{t_m^{s,0}}$) as a function of the root of the mixing time axis is directly proportional to the size of the mobile nanophases.[39,41] The average diameter of these mobile nanodomains (d_{mobile}) can be calculated from $\sqrt{t_m^{s,0}}$ as described in the literature:[37,38]

$$d_{mobile} = \frac{2\epsilon}{\sqrt{\pi}}\sqrt{D_{eff} t_m^{s,0}} \quad (1)$$

where ϵ is the number of orthogonal directions that exchange effectively magnetization between the two different phases. The "geometry parameter", ϵ, is 1 for lamellae, 2 for cylinders, and 3 for spheres; therefore, it strongly influences the calculated diameter of mobile nanodomains. $\sqrt{D_{eff}}$ is defined as the geometric average of $\sqrt{D_{mobile}}$ and $\sqrt{D_{rigid}}$ divided by the arithmetic average of their square roots:[39,41]

$$\sqrt{D_{eff}} = \frac{\sqrt{D_{mobile}}\sqrt{D_{rigid}}}{(\sqrt{D_{mobile}} + \sqrt{D_{rigid}})/2} \quad (2)$$

The value for the rigid phase spin diffusion coefficient of D_{rigid} = 0.8 nm²/ms has been determined previously in the literature.[39,41] The spin diffusion coefficient of the mobile nanophase (D_{mobile}) can be determined from spin-echo measurements of transverse relaxation rate T_2^{-1} (in hertz) by an empirically established relation for small diffusion coefficients (T_2^{-1} < 1000 Hz):[38]

$$D_{mobile}(T_2^{-1}) = (8.2 \times 10^{-6} T_2^{-1.5} + 0.007)\ [\mathrm{nm^2/ms}] \quad (3)$$

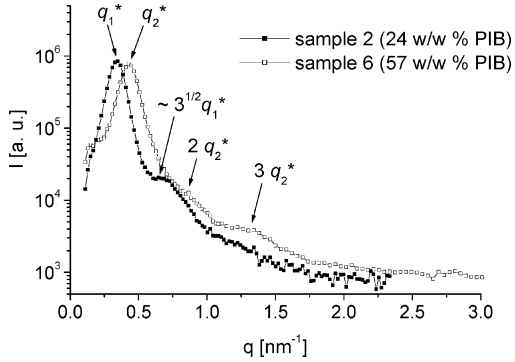

Figure 6. Small-angle X-ray scattering (SAXS) traces of 24% and 57% w/w PIB containing PHEMA-*l*-PIB amphiphilic conetworks. The first-order peaks (q^*) correlate with a periodicity of 18.5 and 14.6 nm in these samples. The appearance of higher small intensity peaks indicates a short-range ordering. The presumed approximate structure is lamellar for sample 6 and simple cubic for sample 2.

For all PHEMA-*l*-PIB samples, the measured T_2^{-1} values are about 390 Hz, which results in a value of $D_{\text{mobile}} = 0.07$ nm^2/ms according to eq 3. Because of a similar dynamic contrast for all samples, the diffusion coefficient D_{mobile} of the mobile PIB phase is nearly independent of the mobile/rigid polymer content of the conetworks.

There is no exact information available concerning the shape of the mobile (PIB) nanophases in amphiphilic conetworks (see also next section), and ^{1}H spin diffusion NMR results will not provide information about the form of PIB nanophases. This question can be tackled by using complementary scattering techniques. It is not even clear whether only a single, well-defined morphology dominates the local structure of the PHEMA-*l*-PIB conetworks. It is possible to approximate the value of ϵ from the spin diffusion curves in combination with SAXS measurements (see later in this article) and to assume a morphology in analogy with phase existing in diblock copolymers.[55,60,61] Therefore, the results of the spin diffusion measurements toward the size of the PIB nanophase will be discussed in the context of the SAXS measurements.

SAXS Measurements. Small-angle X-ray scattering (SAXS) supplies information about the distance of separated nanophases and the symmetry of the nanodomain structure. Figure 6 depicts the SAXS traces of two samples with different PIB content. The two samples have different structures: in the conetwork containing 24% w/w PIB, the PIB nanophases are separated in the PHEMA matrix, while the conetwork containing 57% w/w PIB is co-continuous for both components.[57] The clearly visible single peaks can be related to the long periods (smallest repeat units). In these cases the scattering centers are the separated nanophases, and the distance between centers of mass of two identical neighboring nanophases can be calculated from the first-order peak. $q^* = 0.34$ nm^{-1} for 24% w/w and $q^* = 0.43$ nm^{-1} for 57% w/w PIB containing sample were found, which result in 18.5 and 14.6 nm as the long periods, respectively. Additionally, small intensity peaks of higher order are present, indicating that the samples have only weak long-range order. The positions of the higher order peaks are different, suggesting different structures in the two samples. The sample containing 57% w/w PIB has small intensity higher order peaks at $2q^*$ and $3q^*$ (see Figure 6), which indicates that the conetwork has an approximately lamella-like ordered structure. The second-order peak has a very weak intensity, in good agreement with the expectation for a sample's composition of nearly 0.5 volume ratio. This finding agrees with the results of small-angle neutron scattering (SANS) measurements on a similar system.[31] The other sample (see Figure 6), which contains 24% w/w PIB, has a different morphology as indicated via its SAXS trace. The second-order peak at about $\sqrt{3}q^*$ is observable, but there are no higher order peaks or their intensities are too low. This sample also has a weakly ordered local structure, but the SAXS trace is not sufficient for a definite assignment (see detailed discussion in the next section). AFM pictures[57] taken on the sample containing 24% w/w PIB are consistent with a structure where the PIB nanophases are locally ordered independent spheres as predicted by the theory for diblock copolymers, which might serve as guidelines.[55,60,61]

Size of the PIB Nanophases. As described in the Experimental Section, during the synthesis of the conetworks, the polymer chains are miscible; therefore, the arrangement of the cross-linked PIB and protected PHEMA chains is assumed to be statistical. After the removal of the protecting groups, the covalently bonded chains cannot rearrange to generate the long-range ordered structures as predicted for diblock copolymers.[55] Because of the covalently bonded network structure, the macroscopic phase separation is excluded and the local relaxation of the nanostructure is also strongly hindered. The chemically bonded network structure allows only local ordering and limits long-range order. The immiscible nanophases adopt similar structures as diblock copolymers, but the arrangements prevail only on short length scale. As the AFM[57] pictures of these amphiphilic conetworks show, the number of the repeat units (e.g. spheres or lamellae) is not larger than 10−20. The amphiphilic conetworks have a complex nanomorphology, and it depends strongly on the composition, as indicated by AFM and TEM investigations.[57] In this work, the PIB nanophases are assumed to be spheres of several nanometers in size within the PHEMA matrix when the PIB content is very low. In the middle composition range (about 50% w/w PIB content) the morphology is locally ordered layered-like (lamellar) as indicated by X-ray data, and at very high PIB content PHEMA spheres appear. The possibility of a more complex equilibrium (gyroid, hexagonal) and nonequilibrium (hexagonal perforated lamellar, hexagonally modulated lamellar) structures[62,63] can neither be confirmed nor excluded using the here presented NMR and X-ray data.

Figure 7 shows the average size of PIB domains calculated from the ^{1}H spin diffusion solid-state NMR and from the SAXS measurements. The "geometry parameter" ϵ in eq 1 is important for the correct interpretation of the NMR results, and from the SAXS, SANS,[31] and AFM[57] experiments, their value can be estimated. In the co-continuous range (over 50% w/w PIB content) the amphiphilic conetworks have a locally ordered lamellar structure, and in this case, ϵ is assumed to be equal to 1. This results in an average thickness of PIB lamellae of 7.5−10 nm. If the PIB content is very low, then the PIB nanophases are most probably spheres ($\epsilon = 3$) and their average diameter reaches up to 15 nm. The transition between the "distinct spheres" and the lamellar structure is most

Table 3. Summary of SAXS and ^{1}H Spin Diffusion NMR Measurements for Two Selected Compositions[a]

sample no.	PIB content [% w/w]	vol fraction of PIB	d_{long} calculated from composition and ^{1}H spin diffusion NMR [nm]					long period by SAXS [nm]	size of PIB nanophase [nm]	
			$\epsilon = 3$			$\epsilon = 2$	$\epsilon = 1$			
			sc	bcc	fcc	hexagonal	lamellar		NMR	SAXS
2	24	0.27	**18.2**	19.9	22.0	20.3	17.8	18.5	14.6	14.8
6	57	0.61	20.1	21.9	24.3	19.9	**11.8**	14.6	7.2	8.9

[a] The long period d_{long} was calculated from ^{1}H spin diffusion NMR results with different "geometry parameter" ϵ. The suggested structures are simple cubic ordered PIB spheres in a PHEMA matrix for sample 2 and lamella-like ordering for sample 6 (the best agreeable calculated long periods with the measured values are indicated with bold numbers).

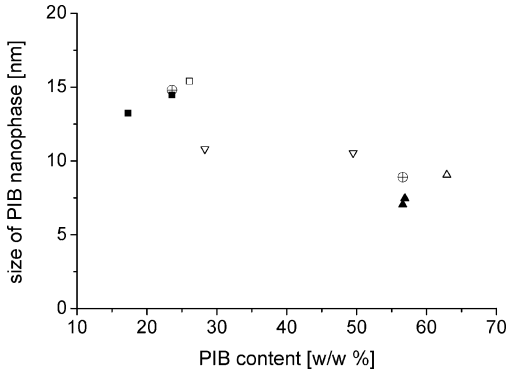

Figure 7. Average size of mobile-phase (PIB) nanodomains vs composition as measured by spin diffusion experiments utilizing different ϵ values. SAXS experiments for two selected samples were included, and the stoichiometric content was used to calculate the PIB domain size (circle with cross inside). For well-established morphologies ϵ values with full symbols are used; for less defined morphologies ϵ values with open symbols are used (up triangle for $\epsilon = 1$, down triangle for $\epsilon = 2$, and square for $\epsilon = 3$).

probably continuous, so the ϵ value decreases continuously from 3 to 1. The average diameter of PIB nanophases in the intermediate range is between 7.5 and 15 nm, and the distribution of their size and shape seems to be very broad.

From the first-order peak (q^*) of the SAXS traces, the periodicity (long period) can be calculated (Table 3). For the sample containing 24% w/w PIB q^* is 0.34 nm^{-1}, which results in a distance of 18.5 nm as a long period. As mentioned in the previous section, the sample has a weak short-range ordering, but the SAXS trace alone is not sufficient to determine the structure. For the sample with 57% w/w PIB content, the first-order peak at 0.43 nm^{-1} results in a periodicity of 14.6 nm (long period), and the appearance of higher order peaks at $2q^*$ and $3q^*$ indicates that the sample has a lamella-like structure. The NMR results and composition data exclude several types of local ordering, and a possible structure will now be discussed.

From the NMR measurements, the average size of PIB nanophase is known, and the volume fraction of the components can be calculated from the composition data ($\rho_{PIB} = 0.92$ g/cm^3; $\rho_{PHEMA} = 1.07$ g/cm^3). In Table 3 the calculated long periods for some given simple symmetries (simple cubic, sc; body-centered cubic, bcc; face-centered cubic, fcc; hexagonal; lamellar) are compared with the SAXS measured long periods. For sample 2 (24% w/w PIB), the simple cubic, and for sample 6 (57% w/w PIB), the lamella-like ordered morphology show the best agreement between the measured and the calculated values of the long period. The q positions of the Bragg peaks for these ideal and pure structures vary as follows: for sc $q^*:\sqrt{2}q^*:\sqrt{3}q^*:2q^*$; for bcc $q^*:\sqrt{2}q^*:\sqrt{3}q^*:2q^*$; for fcc $q^*:\sqrt{2}q^*:2q^*:\sqrt{11/2}q^*$; for hexagonal $q^*:\sqrt{3}q^*:2q^*:\sqrt{7}q^*$; for lamellar $q^*:2q^*:3q^*:4q^*$. In the SAXS trace of sample 6 the first three peaks at 1, 2, $3q^*$ can be observed according to lamellar morphology. For sample 2 only the first- and third-order peaks at q^*, $\sqrt{3}q^*$ are clearly observable. The second-order peak at $\sqrt{2}q^*$ cannot be identified on the tail of the broad q^* because of its small intensity. The values for sample 2 agree very well, but for sample 6 the thickness of PIB lamellae calculated from SAXS is larger than the NMR measured size (Table 3). The PIB layer thickness was determined from NMR with $\epsilon = 1$, which is fully justified if the lamellae have an infinite grain size. If their grain size is "finite", the effective spin diffusion can occur in more than one dimension, i.e., mainly perpendicular to the lamellae but also parallel to them at the boundaries. Thus, the "geometry parameter" should then be chosen between 1 and 2. This can explain the difference between the SAXS results and the NMR experiments.

As described in the experimental part, the chain lengths of the PIB chains are the same ($M_w \cong 5000$ g/mol, contour length of about 25 nm) for all conetwork samples. The radius of the statistical coil of one PIB chain is only about 3 nm, so we can conclude that a PIB nanosphere with diameter of 10−15 nm is composed of about 60−180 chains, but we have no detailed information about the conformation and dynamics of chains within the conetwork. Nevertheless, the strong separation and the difference of the Gaussian chain size and the detected domain size suggest a highly stretched conformation. The effect of the conformation (γ-gauche effect) on the ^{13}C chemical shift of PIB methyl and methylene carbons was already analyzed by ab initio calculations and ^{13}C CP/MAS measurements.[64,65] Preliminary measurements on the conetwork samples carried out at low temperature reveal the isotropic chemical shift of the methylene carbon. The determination of the contribution of the conformations, however, is difficult because of spectral overlap with other carbon signals from the PHEMA (−O−CH_2−, −CH_2−OH, and the tertiary carbon). This study therefore requires further investigation, e.g., by establishing adequate filtering of the PHEMA signals (T_1, T_2 filter) and is currently under investigation.

Conclusions. PHEMA-*l*-PIB amphiphilic conetworks with different PIB contents were synthesized. The conetworks were investigated by DSC, ^{1}H spin diffusion solid-state NMR, and SAXS. Nanophase-separated structures were found for both phases in all of the conetworks without detectable interphase between them as indicated by ^{1}H spin diffusion solid-state NMR data. At lower PIB content, the PIB nanodomains (spheres) are segregated from each other in a PHEMA matrix, most probably in a simple cubic structure, and the average diameter of the spheres is about 15 nm with 18−20 nm

long period. At higher PIB contents (>50% w/w) the structure of the conetworks is co-continuous, and the different phases form lamellae on the local scale; the size of the PIB domains is about 7.5−10 nm with 15−20 nm long period. These structures only exist on the short range, the number of repeat units (e.g. spheres or lamellae) is not more than 10−20 unit cells. In the intermediate composition range, the morphology is more complicated, and most probably the transition between the "separated" and co-continuous structure is gradual with increasing PIB content.

Acknowledgment. This study was supported by the National Scientific Research Fund (OTKA F031901), Alexander von Humboldt Foundation, and Marie Curie Fellowship of the European Community programme Improving Human Research Potential and the Socio-economic Knowledge Base under Contract HPMF-CT-2001-01202 for A. Domján. We are indebted to Dr. Hedvig Medzihradszky-Schweiger, Dr. Márta Szesztay, Erzsébet Tyroler (Budapest), and Uta Pawelzik (Mainz) for the characterization of the conetworks, to Dr. Jochen Gutmann and Michael Bach (both Mainz) for their help with SAXS measurements and its interpretation, to Dr. Lothar Brombacher for his support in simulating the spin diffusion curves, and to Dr. Robert Graf (both Mainz) for helpful discussions on NMR techniques. We also thank Uli Wiesner (Cornell University) for his support during the early stages of this work.

References and Notes

(1) Hillmeyer, M. A.; Bates, F. S.; Ryan, A.; Fairclough, P.; Almdal, K.; Mortensen, K. *Science* **1996**, *271*, 976.
(2) Stupp, S. I.; LeBonheur, V.; Walker, K.; Li, L. S.; Huggins, K.; Keser, M.; Amstutz, A. *Science* **1997**, *276*, 384.
(3) Park, M.; Harrison, C.; Chaikin, P. M.; Register, R. A.; Adamson, D. H. *Science* **1997**, *276*, 1401.
(4) Goldacker, T.; Abetz, V.; Stadler, R.; Erukhimovich, I.; Leibler, L. *Nature (London)* **1999**, *398*, 137.
(5) Hadjichristidis, N. *J. Polym. Sci. Part A: Polym. Chem.* **1999**, *37*, 857.
(6) Goethals, E. J., Ed.; *Telechelic Polymers*; CRC Press: Boca Raton, FL, 1989.
(7) Iván, B.; Kennedy, J. P.; Mackey, P. W. *Polym. Prepr.* **1990**, *31*, 217.
(8) Iván, B. *Macromol. Symp.* **1994**, *88*, 201.
(9) Iván, B.; Kennedy, J. P. *Ind. J. Technol.* **1993**, *31*, 183.
(10) Iván, B. *Makromol. Chem., Macromol. Symp.* **1993**, *75*, 181.
(11) Erdödi, G.; Janecska, Á.; Iván, B. Novel Intelligent Amphiphilic Conetworks. In *Wiley Polymer Networks Group Reviews;* Stokke, B. T., Elgsaeter, A., Eds.; Wiley: New York, 1999; Vol. 2, p 73.
(12) Kennedy, J. P.; Fenyvesi, G.; Na, S.; Keszler, B.; Rosenthal, K. S. *Des. Monomers Polym.* **2000**, *3*, 113.
(13) Park, D.; Keszler, B.; Galiatsatos, V.; Kennedy, J. P. *J. Appl. Polym. Sci.* **1997**, *66*, 901.
(14) Park, D.; Keszler, B.; Galiatsatos, V.; Kennedy, J. P.; Ratner, B. D. *Macromolecules* **1995**, *28*, 2595.
(15) Iván, B.; Feldthusen, J.; Müller, A. H. E. *Macromol. Symp.* **1996**, *102*, 81.
(16) Süvegh, K.; Domján, A.; Vankó, Gy; Iván, B.; Vértes, A. *Macromolecules* **1998**, *31*, 7770.
(17) Domján, A.; Iván, B.; Süvegh, K.; Vértes, A. *Mater. Sci. Forum* **2001**, *363−365*, 365.
(18) Domján, A.; Iván, B.; Süvegh, K.; Vankó, Gy.; Vértes, A. *Polym. Mater. Sci. Eng.* **1998**, *79*, 455.
(19) Künzler, J.; Ozark, R. *J. Appl. Polym. Sci.* **1995**, *55*, 611.
(20) Lai, Y. C.; Valint, P. L., Jr. *J. Appl. Polym. Sci.* **1996**, *61*, 2051.
(21) Scherble, J.; Thomann, R.; Iván, B.; Mülhaupt, R. *J. Polym. Sci., Part B: Polym. Phys.* **2001**, *39*, 1429.
(22) Christova, D.; Velichkova, R.; Goethals, E. J.; Du Prez, F. E. *Polymer* **2002**, *43*, 4584.
(23) Rimmer, S.; Tattersall, P.; Ebdon, J. R.; Fullwood, N. *React. Funct. Polym.* **1999**, *41*, 177.
(24) Simmons, M. R.; Yamasaki, E. N.; Patrickios, C. S. *Macromolecules* **2000**, *33*, 3176.
(25) Triftaridou, A. I.; Hadjiyannakou, S. C.; Vamvakaki, M.; Patrickios, C. S. *Macromolecules* **2002**, *35*, 2506.
(26) Guan, Y.; Zhang, W.; Wan, G.; Peng, Y. *J. Polym. Sci., Part A: Polym. Chem.* **2000**, *38*, 3812.
(27) Guan, Y.; Jiang, W.; Zhang, W.; Wan, G.; Peng, Y. *J. Polym. Sci., Part B: Polym. Phys.* **2001**, *39*, 1784.
(28) Iván, B.; Kennedy, J. P.; Mackey, P. W. In *Polymeric Drugs and Drug Delivery Systems*; Dunn, R. L., Ottenbrite, R. M., Eds.; ACS Symp. Ser. Vol. 469; American Chemical Society: Washington, DC, 1991; p 203.
(29) Iván, B.; Kennedy, J. P.; Mackey, P. W. In *Polymeric Drugs and Drug Delivery Systems*; Dunn, R. L., Ottenbrite, R. M., Eds.; ACS Symp. Ser. Vol. 469; American Chemical Society: Washington, DC, 1991; p 194.
(30) Chen, D.; Kennedy, J. P.; Allen, A. J. *J. Macromol. Sci., Chem.* **1988**, *A25*, 389.
(31) Iván, B.; Almdal, K.; Mortensen, K.; Johannsen, I.; Kops, J. *Macromolecules* **2001**, *34*, 1579.
(32) Adriaensens, P.; Storme, L.; Carleer, R.; Gelan, J.; Du Prez, F. E. *Macromolecules* **2002**, *35*, 3965.
(33) Chen, D.; Kennedy, J. P.; Kory, M. M.; Ely, D. J. *J. Biomed. Mater. Res.* **1989**, *23*, 1327.
(34) Keszler, B.; Kennedy, J. P.; Ziats, N. P.; Brunstedt, M. R.; Stack, S.; Yun, J. K.; Anderson, J. M. *Polym. Bull.* **1992**, *29*, 681.
(35) Keszler, B.; Kennedy, J. P.; Mackey, P. W. *J. Controlled Release* **1993**, *25*, 115.
(36) Iván, B.; Kennedy, J. P.; Mackey, P. M. U.S. Patent 5,073,-381, 1991.
(37) Mellinger, F.; Wilhelm, M.; Spiess, H. W.; Baumstark, R.; Haunschild, A. *Macromol. Chem. Phys.* **1999**, *200*, 719.
(38) Mellinger, F.; Wilhelm, M.; Spiess, H. W. *Macromolecules* **1999**, *32*, 4686.
(39) Clauss, J.; Schmidt-Rohr, K.; Spiess, H. W. *Acta Polym.* **1993**, *44*, 1.
(40) Diez-Pena, E.; Quijada-Garrido, I.; Barrales-Rienda, J. M.; Wilhelm, M.; Spiess, H. W. *Macromol. Chem. Phys.* **2002**, *203*, 491.
(41) Schmidt-Rohr, K.; Spiess, H. W. *Multidimensional Solid-State NMR and Polymers*; Academic Press: San Diego, CA, 1994.
(42) Hou, S. S.; Graf, R.; Spiess, H. W.; Kuo, P. L. *Macromol. Rapid Commun.* **2001**, *22*, 1386.
(43) Adriaensens, P.; Storme, L.; Carleer, R.; Gelan, J. *Macromolecules* **2002**, *35*, 3965.
(44) VanderHart, D. L.; McFadden, G. B. *Solid State Nucl. Magn. Reson.* **1996**, *7*, 45.
(45) VanderHart, D. L. *Makromol. Chem., Macromol. Symp.* **1990**, *34*, 125.
(46) Cheung, T. T. P. *J. Phys. Chem. B* **1999**, *103*, 9423.
(47) Egger, N.; Schmidt-Rohr, K.; Blümlich, B.; Domke, W.-D.; Stapp, B. *J. Appl. Polym. Sci.* **1992**, *44*, 289.
(48) Cai, W. Z.; Schmidt-Rohr, K.; Egger, N.; Gerharz, B.; Spiess, H. W. *Polymer* **1993**, *34*, 267.
(49) Goldman, M.; Shen, L. *Phys. Rev.* **1966**, *144*, 321.
(50) Jia, X.; Wolak, J.; Wang, X.; White, J. L. *Macromolecules* **2003**, *36*, 712.
(51) Wang, X.; White, J. L. *Macromolecules* **2002**, *35*, 3795.
(52) Carr, H. Y.; Purcell, E. M. *Phys. Rev.* **1954**, *94*, 630.
(53) Meiboom, S.; Gill, D. *Rev. Sci. Instrum.* **1958**, *29*, 6881.
(54) Gedde, U. W. *Polymer Physics*; Kluwer Academic Publishers: Dordrecht, 1995; p 70.
(55) Hamley, I. W. *The Physics of Block Copolymers*; Oxford University Press: Oxford, 1998.
(56) *Polymer Data Handbook*; Mark, J. E., Eds.; Oxford University Press: New York, 1999.
(57) Scherble, J.; Thomann, R.; Iván, B.; Erdödi, G.; Domján, A.; Müllhaupt, R., to be submitted to *Macromolecules*.
(58) Dollase, T.; Graf, R.; Heuer, A.; Spiess, H. W. *Macromolecules* **2001**, *34*, 298.
(59) Landfester, K.; Spiess, H. W. *Acta Polym.* **1998**, *49*, 451.
(60) Bates, F. S. *Science* **1991**, *251*, 898.
(61) Leibler, L. *Macromolecules* **1980**, *13*, 1602.
(62) Hajduk, D. A.; Takenouchi, H.; Hillmeyer, M. A.; Bates, F. S.; Vigild, M. E.; Almdal, K. *Macromolecules* **1997**, *30*, 3788.
(63) Vigild, M. E.; Almdal, K.; Mortensen, K.; Hamley, I. W.; Fairclough, J. P. A.; Ryan, A. J. *Macromolecules* **1998**, *31*, 5702.
(64) Born, R.; Spiess, H. W. *Macromolecules* **1994**, *27*, 1500.
(65) Born, R.; Spiess, H. W. *NMR Basic Principles and Progress 35*; Seeling, J., Ed.; Springer-Verlag: Berlin, Heidelberg, 1997.

MA034891H